# Backbone Dynamics of the C-Terminal Domain of *Escherichia coli* Topoisomerase I in the Absence and Presence of Single-Stranded DNA

Liping Yu,[‡] Chang-Xi Zhu,[§] Yuk-Ching Tse-Dinh,[§] and Stephen W. Fesik*,[‡]

*Pharmaceutical Discovery Division, D47G, AP10, Abbott Laboratories, Abbott Park, Illinois 60064, and Department of Biochemistry and Molecular Biology, New York Medical College, Valhalla, New York 10595*

*Received February 29, 1996; Revised Manuscript Received May 13, 1996*[⊗]

ABSTRACT: The backbone dynamics of the C-terminal DNA-binding domain of *Escherichia coli* topoisomerase I has been characterized in the absence and presence of single-stranded DNA by NMR spectroscopy. $^{15}$N spin−lattice relaxation times ($T_1$), spin−spin relaxation times ($T_2$), and heteronuclear NOEs were determined for the uniformly $^{15}$N-labeled protein. These data were analyzed by using the model-free formalism to derive the model-free parameters ($S^2$, $\tau_e$, and $R_{ex}$) for each backbone N−H bond vector and the overall molecular rotational correlation time ($\tau_m$). The molecular rotational correlation time $\tau_m$ was determined to be 7.49 ± 0.36 ns for the free and 12.7 ± 1.07 ns for the complexed protein. Several residues were found to be much more mobile than the average, including 11 residues at the N-terminus, 2 residues at the C-terminus, and residues 25 and 31−35 which are located in a region of the protein that binds to DNA. The binding of ssDNA to the free protein causes a slight increase in the order parameters ($S^2$) for a small number of residues and a slight decrease in the order parameters ($S^2$) for the majority of the residues. In particular, upon binding to ssDNA, the mobility of the first α-helix and the two $\beta$-sheets was slightly increased, and the mobility of a few specific residues in the loops/turns was restricted. These results differ from the previous studies on the backbone dynamics of molecular complexes in which reduced mobilities were typically observed upon ligand binding.

Dynamics can markedly influence the biological activity and function of proteins. Knowledge of the changes in protein dynamics that occur upon ligand binding is especially important for understanding the processes of molecular interactions. However, only a few studies have addressed this issue. Earlier work on ligand-induced changes in protein dynamics includes NMR[1] studies of staphylococcal nuclease in the presence and absence of a small inhibitor (pdTp) and $Ca^{2+}$ (Nicholson et al., 1992), apo- and $Cd^{2+}$-loaded calbindin (Akke et al., 1993), FK506 binding protein free and when bound to FK506 (Cheng et al., 1993, 1994), ribonuclease T1 in the presence and absence of a small inhibitor 2′GMP (Fushman et al., 1994), and the SH2 domain of PLC$_\gamma$1C in the presence and absence of a bound phosphopeptide (Farrow et al., 1994). In the first four studies, an increase in the order parameters corresponding to a stiffening of the structures was observed upon ligand binding. In contrast, most of the amino acid residues of the SH2 domain that interact with the phosphopeptide became more flexible upon ligand binding and exhibited reduced order parameters.

Recently, we determined the three-dimensional structure of the C-terminal single-stranded DNA-binding domain of *Escherichia coli* topoisomerase I using NMR spectroscopy (Yu et al., 1995). This domain is responsible for enhancing the binding to DNA and improving the enzyme's ability to relax negatively supercoiled DNA under high salt conditions (Beran-Steed et al., 1989; Tse-Dinh, 1994). Here we report on the backbone dynamics of the C-terminal single-stranded DNA-binding domain of *E. coli* topoisomerase I in the absence and presence of a 12-mer ssDNA that was previously shown to bind to this protein (Yu et al., 1995). The goals of this study were to determine whether any motional differences exist between the two subdomains $(\beta\beta\beta\beta\alpha)_2$ which might be important for DNA binding, to identify those regions of the protein that are inherently mobile or rigid, and, most importantly, to determine the effects on the motional properties of the protein upon complex formation with ssDNA.

## MATERIALS AND METHODS

*NMR Sample Preparation*. The 14 kDa fragment of *E. coli* DNA topoisomerase I (residues 745−865) was cloned, expressed, and purified as previously described (Zhu et al., 1995). Uniformly $^{15}$N-labeled protein was prepared from bacteria grown in a minimal medium containing $^{15}NH_4Cl$. The protein was purified by phosphocellulose P11 ion exchange, ssDNA agarose affinity, and reverse-phase HPLC chromatography followed by refolding from 6 M urea at 4 °C by dialysis against a solution containing 200 mM potassium phosphate (pH 6.5) and 5 mM dithiothreitol. The NMR sample of the free protein was prepared at a protein concentration of 3 mM in a buffer solution containing 5 mM dithiothreitol-$d_{10}$ and 200 mM potassium phosphate (pH 6.5). The only difference for the sample of the protein/DNA complex was the addition of a 5-fold excess of 12-mer ssDNA d(ACGACAGGCTAC) and the reduction of potassium phosphate to 10 mM in order to increase the binding affinity (Yu et al., 1995).

* To whom correspondence should be addressed.
‡ Abbott Laboratories.
§ New York Medical College.
⊗ Abstract published in *Advance ACS Abstracts,* July 15, 1996.
[1] Abbreviations: 1D, one dimensional; 2D, two dimensional; NMR, nuclear magnetic resonance; NOE, nuclear Overhauser effect; HSQC, heteronuclear single-quantum coherence; TPPI, time-proportional phase incrementation; HPLC, high-pressure liquid chromatography; CPMG, Carr−Purcell−Meiboom−Gill multipulse sequence; RMSD, root mean square deviation; kDa, kilodalton; ssDNA, single-stranded DNA.

S0006-2960(96)00507-7 CCC: $12.00 

*NMR Measurements*. All NMR experiments were recorded at 30 °C on a Bruker AMX 500 MHz spectrometer. NMR spectra were processed and analyzed using in-house written software on Silicon Graphics computers.

$^{15}$N $T_1$ and $T_2$ were recorded as previously described (Stone et al., 1992; Barbato et al., 1992). $^{15}$N NOE spectra were acquired with sensitivity enhancement by using gradients as described by Farrow et al. (1994). All the experiments were recorded with a sweep width of 8333 Hz in the $F_2$ dimension with the $^1$H carrier set to the water signal and a sweep width of 2083 Hz in the $F_1$ dimension. The spectra were acquired in the phase-sensitive mode using the States−TPPI methods (Marion et al., 1989) for the quadrature detection in the $F_1$ dimension. Water suppression in the $^{15}$N $T_1$ and $T_2$ experiments was achieved by using a high-power spin-locking purge pulse (Messerle et al., 1989). A total of 160 ($t_1$) × 2048 ($t_2$) complex points were recorded with 8 scans per increment for both $T_1$ and $T_2$ experiments. The heteronuclear NOE experiments were collected with 16 scans per increment. $^{15}$N decoupling during data acquisition was accomplished using a WALTZ decoupling scheme (Shaka et al., 1983).

For the $T_1$ and $T_2$ experiments, a recycle time of 3.3 s was used between acquisitions to ensure sufficient recovery of the $^1$H magnetization. For the NOE measurements, a recycle time of 4.0 s (approximately 5 times the longest $^{15}$N $T_1$) was used between scans to ensure the maximal development of NOEs before acquisition. The final data sets consisted of 1024 ($t_1$) × 1024 ($t_2$) real data points after zero-filling and Fourier transformation.

*Determination of $^{15}$N $T_1$, $T_2$, and Heteronuclear NOEs*. The longitudinal and transverse relaxation times, $T_1$ and $T_2$, were obtained from a three- or two-parameter monoexponential nonlinear least squares fit to the cross peak heights versus relaxation delays in the $T_1$ and $T_2$ experiments (Stone et al., 1992; Barbato et al., 1992). For the uncomplexed sample, the uncertainties in the $T_1$ and $T_2$ measurements were estimated by performing Monte Carlo simulations based upon the estimated errors in the measured peak heights (Palmer et al., 1991). For the protein/DNA complex, duplicate data sets were collected for both $T_1$ and $T_2$ and were used to report their average values and standard deviations.

For both the free and complexed proteins, the steady-state $^1$H−$^{15}$N NOE of each residue was calculated for each data set as the ratio of the peak height in the spectrum recorded with proton saturation to that in the spectrum recorded without proton saturation during the NOE delay period. Two duplicate data sets were collected for the NOE experiments which were used to calculate their average values and standard deviations.

*Model-Free Calculations*. The spin relaxation of the $^{15}$N nuclei is primarily caused by the dipolar interaction between the $^{15}$N nucleus and the attached protons and the chemical shift anisotropy. $^{15}$N relaxation rates and NOEs are dependent on the spectral density function describing the contributions of five distinct frequencies (0, $\omega_N$, $\omega_H + \omega_N$, $\omega_H$, $\omega_H - \omega_N$) to the motion of the individual amide bond vectors. For a two-spin $^{15}$N−$^1$H system, the relaxation times $T_1$ and $T_2$ and the steady-state NOE can be expressed as (Abragam, 1961; Peng & Wagner, 1992a,b; Stone et al., 1992)

$$\frac{1}{T_1} = \frac{d^2}{4}[3J(\omega_N) + J(\omega_H - \omega_N) + 6J(\omega_H + \omega_N)] + c^2 J(\omega_N) \quad (1)$$

$$\frac{1}{T_2} = \frac{d^2}{8}[4J(0) + 3J(\omega_N) + J(\omega_H - \omega_N) + 6J(\omega_H) + 6J(\omega_H + \omega_N)] + \frac{c^2}{6}[4J(0) + 3J(\omega_N)] + R_{ex} \quad (2)$$

$$\mathrm{NOE} = 1 + \frac{d^2}{4}T_1\frac{\gamma_H}{\gamma_N}[6J(\omega_H + \omega_N) - J(\omega_H - \omega_N)] \quad (3)$$

in which $d = (h/2\pi)(\mu_o/4\pi)\gamma_H\gamma_N\langle r^{-3}\rangle$ and $c = (1/3)^{1/2}\omega_N(\sigma_{||} - \sigma_\perp)$. The symbols in these equations have their usual meanings (Abragam, 1961; Stone et al., 1992; Farrow et al., 1994).

In the absence of any assumption about the form of the spectral density function, the three experiments ($T_1$, $T_2$, NOE) do not provide enough information to enable direct determination of the spectral density function at all five frequencies. Rather than performing additional relaxation measurements as described by Peng and Wagner (1992a,b) to map all five spectral density functions, one may describe the spectral density by using a simpler model-free formalism for an isotropically tumbling protein (Lipari & Szabo, 1982a,b; Clore et al., 1990) as follows:

$$J(\omega) = \frac{2}{5}\left[\frac{S^2\tau_m}{1 + (\omega\tau_m)^2} + \frac{(1 - S^2)\tau}{1 + (\omega\tau)^2}\right] \quad (4)$$

where $1/\tau = 1/\tau_m + 1/\tau_e$.

The model-free approach characterizes both the rate and amplitude of internal motions for individual N−H vectors in terms of the generalized order parameter ($S^2$), the overall rotational correlation time ($\tau_m$), and the effective correlation time ($\tau_e$). The values of the generalized order parameter ($S^2$) may range from 0 (corresponding to completely isotropic motion) to 1 (completely restricted motion). The effective correlation time ($\tau_e$) describes the rate of motion for fluctuation of the amide bond vector occurring on the time scale faster than the overall rotation correlation time ($\tau_m$). Since transverse relaxation times ($T_2$) can also be affected by internal motions occurring on a slower time scale, such as those arising from chemical exchange, the exchange broadening contributing factor, $R_{ex}$, was introduced as a correction factor to the $T_2$ relaxation rate (see eq 2) for the calculation of model-free parameters (Stone et al., 1992; Farrow et al., 1994).

Overall isotropic molecular tumbling for the C-terminal domain of *E. coli* topoisomerase I is assumed in the model-free formalism approach. This assumption is quite reasonable, since the correlation times, $\tau_m$, calculated in the present study for each individual backbone $^{15}$N atom from the $T_1/T_2$ ratios (excluding the N-terminal 11 residues and C-terminal 2 residues) are similar, suggesting isotropic motion. Moreover, on the basis of the recently determined NMR solution structure of this protein (Yu et al., 1995), the ratios of the three coordinate axes are calculated to be 1.00:0.94:0.74, supporting the argument that this protein tumbles isotropically in solution.

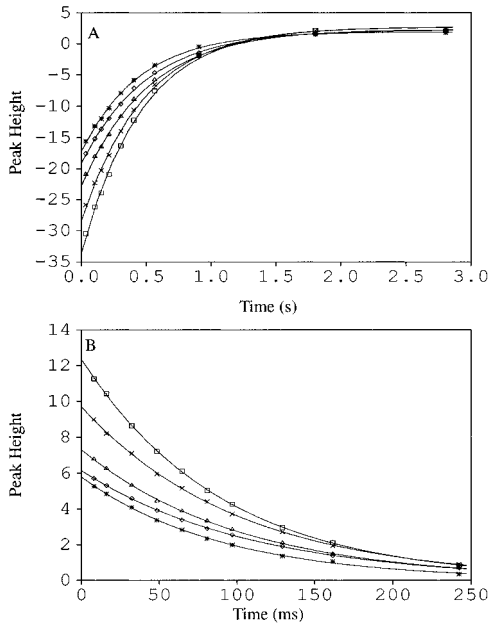


FIGURE 1: Plots of the typical $^{15}N$ $T_1$ (A) and $T_2$ (B) relaxation decay curves of the free form of the C-terminal domain of *E. coli* topoisomerase I: Glu 21 (◇), Asn 41 (*), Ala 74 (□), Val 113 (×), and Val 118 (△). The curves represent the best fits to the three- or two-parameter monoexponential functions. Peak heights are shown on an arbitrary scale.

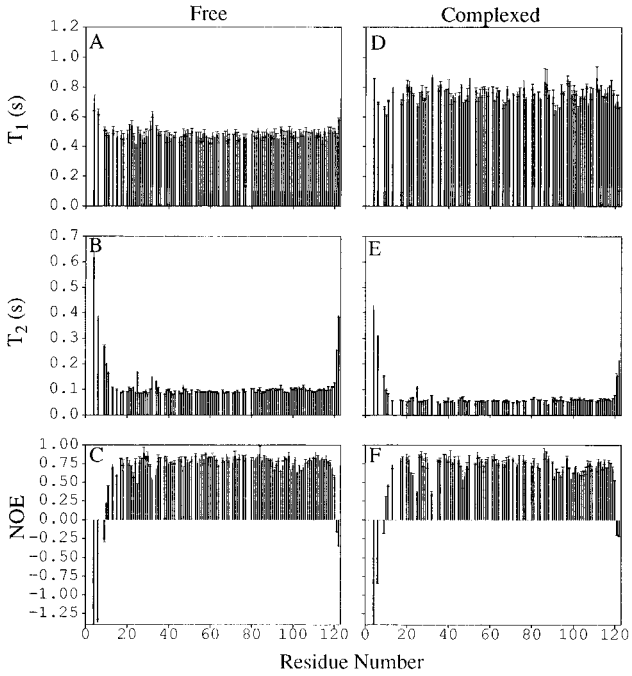


FIGURE 2: Plots of the measured $^{15}N$ relaxation parameters and their uncertainties as a function of residue number for the free and complexed protein. Panels A−C are for the free protein, and panels D−F are for the complexed protein. (A, D) Spin−lattice relaxation time $T_1$. (B, E) Spin−spin relaxation time $T_2$. (C, F) Heteronuclear NOE. Residues for which no results are shown correspond to either proline residues or residues for which NH cross peaks could not observed or severely overlapped.

The model-free parameters ($S^2$, $\tau_e$, and $R_{ex}$) were obtained by substituting eq 4 into eqs 1−3 and followed by minimization of a target function similar to the ones previously described (Stone et al., 1992; Farrow et al., 1994; Zink et al., 1994) by using the experimentally measured $T_1$, $T_2$, and NOE values. Both $\tau_e$ and $R_{ex}$ were included as fitting parameters, and their final values were determined by the global search for the minimum of the target function for each backbone amide. The uncertainties of the model-free parameters were estimated by performing Monte Carlo simulations based on the uncertainties in the measured relaxation parameters (Palmer et al., 1991).

## RESULTS AND DISCUSSION

*Backbone Dynamics of the Free Protein*. The fragment of topoisomerase used in this study contains 122 residues. Among the 110 backbone amide protons (excluding the 11 prolines and N-terminal Met), the amides of Asn 2 and Ala 33 were not observed, and five other residues were excluded from the analysis due to resonance overlap or lack of signal intensity. Thus, quantitative measurements were made for 103 of the amide cross peaks.

Representative plots of the fits for the $^{15}N$ $T_1$ and $T_2$ data are shown in Figure 1. As shown in the plot, good quality fits were obtained for the $T_1$ and $T_2$ data. Figure 2A−C shows the relaxation parameters of the free protein. For most residues, the $T_1$ values lie in the range of 0.43−0.53 s (Figure 2A), and the $T_2$ values ranged from 87 to 110 ms (Figure 2B). The average errors in the calculated $T_1$ and $T_2$ values were 5.0% and 2.4%, respectively. The 11 residues at the N-terminus and 2 residues at the C-terminus of the protein exhibit slow relaxation as evidenced by larger $T_1$ and $T_2$ values which increase toward the ends of the protein. Residues 31−35 which are located in the $\beta$-turn between $\beta$-strands 2 and 3 were also shown to have higher than average $T_1$ and $T_2$ values. The heteronuclear NOEs for most of the residues were found to be in the range of 0.60−0.82 (Figure 2C), indicating that internal motions on the fast (picosecond) time scale are restricted. Exceptions were found for nine of the residues at the N-terminus and two residues at the C-terminus in which the heteronuclear NOEs were found to be negative. In addition, the NOEs for residues 10−15, 21−23, 25, 31−35, 90−95, and 99−107 were all significantly smaller than the average.

The overall rotational correlation time $\tau_m$ was initially estimated to be 7.54 ± 0.37 ns from 44 $T_1/T_2$ ratios of selected residues in the well-defined region of the structure using a previously described approach (Kay et al., 1989; Clore et al., 1990) and subsequently optimized to be 7.49 ± 0.36 ns from the model-free analysis of the data. The value obtained from the model-free analysis, which was subsequently used for the determination of the internal dynamics parameters ($S^2$, $\tau_e$, and $R_{ex}$) for all of the residues in the protein, is in good agreement with those reported previously for proteins of similar size (Kay et al., 1989; Clore et al., 1990; Stone et al., 1992; Cheng et al., 1993; Farrow et al., 1994).

The model-free parameters $S^2$, $\tau_e$, and $R_{ex}$ for the free protein are shown in Figure 3A−C. For most residues, the order parameters ($S^2$) were in the range of 0.75−0.90, indicating that rapid motions on the fast (picosecond) time scale were largely restricted. In contrast, for 11 residues at the N-terminus and 2 residues at the C-terminus, much lower order parameters ($S^2$) were observed that decreased steadily toward their termini (Figure 3A). These results indicate that these segments of the protein have considerable disorder and a high degree of motion on the picosecond to nanosecond time scale. This region (which contains three proline

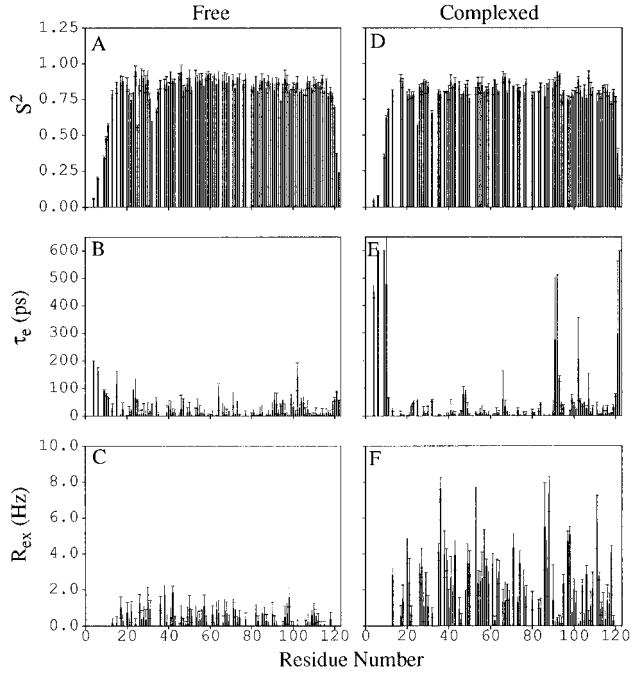


FIGURE 3: Plots of the optimized model-free parameters and their uncertainties as a function of residue number for the free and complexed protein. Panels A−C are for the free protein, and panels D−F are for the complexed protein. (A, D) The generalized order parameter $S^2$. (B, E) The effective correlation time $\tau_e$. (C, F) The chemical exchange line width $R_{ex}$. The standard deviations are estimated from the Monte Carlo simulations.

residues) may function as the linker region between the $Zn^{2+}$-binding domain and the C-terminal domain of *E. coli* topoisomerase I. Ala 25 and residues 31−35 which are located in the $\beta$-turn linking $\beta$-strands 2 and 3 also have significantly lower order parameters ($S^2$) (Figure 3A), indicating that these regions are more mobile than the overall backbone. A significant difference in the order parameters between Ala 25 and its neighboring residues was observed. Such a motional difference between neighboring residues has also been observed previously (Stone et al., 1992; Barbato et al., 1992).

The effective correlation times for internal motions, $\tau_e$, on the other hand, are generally <50 ps (Figure 3B), as in the glucose permease IIA (Stone et al., 1992) and calmodulin (Barbato et al., 1992). Higher (>50 ps) $\tau_e$ values were only found for the 11 residues at the N-terminus, 3 residues at the C-terminus, and residues 15, 23−25, 64, 91, 99, and 102. This result is similar to the N-terminus in glucose permease IIA which showed higher $\tau_e$ values (Stone et al., 1992). Finally, the average $R_{ex}$ exchange line widths for residues with $R_{ex}$ >0 are 0.5 ± 0.4 Hz (Figure 3C), suggesting that motions on the millisecond to microsecond time scale which result in $^{15}N$ line broadening, such as those arising from chemical or conformational exchange processes, are limited in the uncomplexed protein.

The backbone dynamics of the free protein along the peptide chain are summarized in Figure 4 by color-coding the ribbon in the order of increasing mobility: cyan < greenish yellow < pink < magenta. Clearly, the loop/turn residues are generally more mobile than the α-helices and $\beta$-sheets, and the N-terminal $\beta$1 strand and the C-terminal $\beta$8 strand are also more mobile than the rest of the $\beta$-strands. However, not all the loops are mobile. Exceptions include the DNA binding loop (residues 41−46) which contains Phe

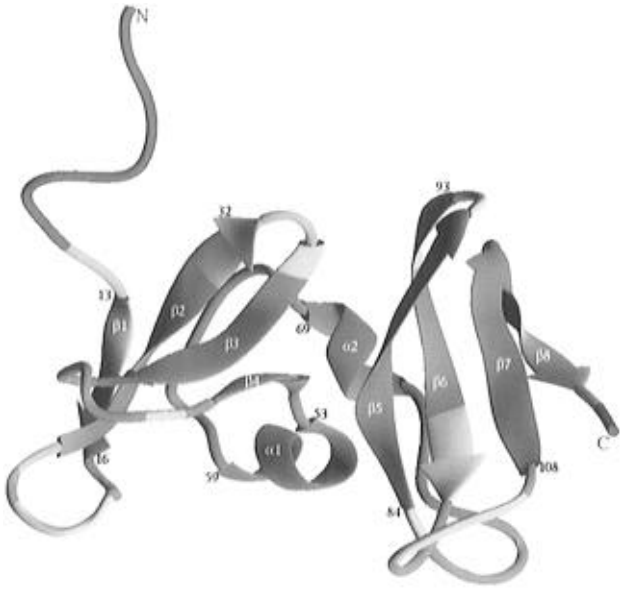


FIGURE 4: Ribbon plot depicting the backbone dynamics of the free form of the C-terminal domain (residues 1−122) of *E. coli* topoisomerase I which consists of eight $\beta$−strands ($\beta$1, 13−16; $\beta$2, 26−32; $\beta$3, 35−40; $\beta$4, 49−51; $\beta$5, 84−90; $\beta$6, 93−99; $\beta$7, 108−113; $\beta$8, 116−119) and two α−helices (α1, 53−59; α2, 69−73). The mobilities of the backbone amides are color-coded on the basis of the values of the order parameters $S^2$: $S^2 \leq 0.5$, magenta; $0.5 < S^2 \leq 0.7$, pink; $0.7 < S^2 \leq 0.82$, greenish yellow; $S^2 > 0.82$, cyan. For Pro as well as some other residues whose relaxation parameters were not determined, the backbone was then color-coded by interpolation based on the order parameters of the neighboring residues.

43, a residue that may form base stacking interactions with DNA and the loop linking the two α-helices (Figure 4).

No obvious and independent motions between the two subdomains of the free protein were observed. This is evidenced by the following: (1) Both of the two central α-helices and the loop which links them are fairly rigid (cyan color in Figure 4). (2) The averaged order parameters ($S^2$) for the N-terminal subdomain (residues 12−64) (0.85 ± 0.08) and the C-terminal subdomain (residues 65−120) (0.84 ± 0.04) are not significantly different, suggesting that they are tumbling together as a whole in solution.

*Backbone Dynamics of the Complexed Protein.* The $^{15}N$ and $^{1}H$ resonances of the backbone amides of the protein complexed to the 12-mer ssDNA d(ACGACAGGCTAC) were assigned from a series of DNA titration experiments by monitoring the $^{1}H/^{15}N$ cross peaks in the HSQC spectra as a function of added DNA. The free and complexed proteins were found to be in fast exchange on the NMR time scale. In addition to 11 Pro residues and 4 residues (Met 1, Asn 2, Gly 3, and Ala 33) whose amide cross peaks were not observed, 16 overlapping amide cross peaks were excluded in the analysis. Thus, quantitative $^{15}N$ $T_1$, $T_2$, and NOE data were obtained for 91 backbone amides in the complexed protein.

Figure 2D−F shows the relaxation parameters for the complexed protein. For most residues, the $^{15}N$ $T_1$, $T_2$, and NOE lie in the ranges of 650−850 ms, 50−70 ms, and 0.60−0.82 ms, respectively (Figure 2D−F). The $^{15}N$ $T_1$ is much longer and $T_2$ is much shorter than those in the free protein. The average errors for the calculated $T_1$, $T_2$, and NOE values were 2.8%, 2.8%, and 4.5%, respectively. The 11 residues at the N-terminus, 2 residues at the C-terminus, Ala 25, and

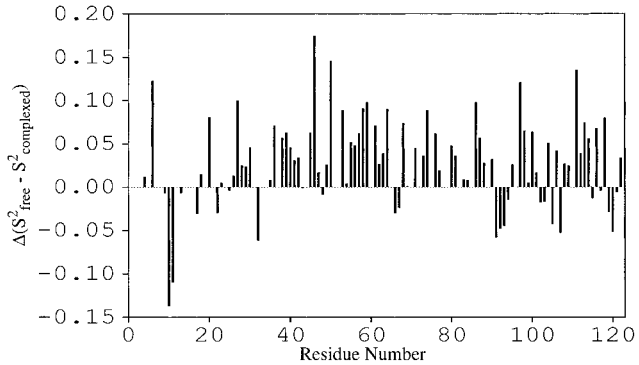


FIGURE 5: Plot of the differences between the order parameters ($S^2$) of the free and complexed C-terminal domain of *E. coli* topoisomerase I. Only the backbone amides whose relaxation parameters were determined in both free and complexed proteins were shown.

Gly 32 clearly exhibit much longer $T_2$ relaxation times and smaller heteronuclear NOEs than average.

The molecular correlation time $\tau_m$ for the complex was initially estimated from $T_1/T_2$ ratios (as in the free protein) to be 13.2 ± 1.06 ns and subsequently optimized to be 12.7 ± 1.07 ns in the model-free analysis. This value was used to determine the model-free parameters $S^2$, $\tau_e$, and $R_{ex}$ for all of the residues. The small spread in the measured $\tau_m$ values as well as the independence of $\tau_m$ values on the orientations of the N−H bond vectors suggests that the motion of the complexed protein is effectively isotropic. The $\tau_m$ value of 12.7 ns at 30 °C for the complexed protein with a total mass of ∼18 kDa (assuming a 1:1 complex) is in good agreement with those reported previously of similar size [∼16 kDa ribonuclease H, 10.4 ns at 26 °C (Powers et al., 1992); ∼19 kDa human granulocyte colony-stimulating factor, 13 ns at 27 °C (Zink et al., 1994)].

Figure 3D−F shows the model-free parameters of the complexed protein. The 11 residues at the N-terminus, 2 residues at the C-terminus, and Ala 25 and Gly 32 had much lower order parameters ($S^2$) than average, indicating that these segments of the protein are more mobile than the overall backbone. The effective correlation times $\tau_e$ (>50 ps) were found for a number of residues located either in loops or at the ends of $\beta$-strands. In particular, the N-terminal residues 1−10, the C-terminal residues 121−122, and the loop residues 91−92 and 102 exhibited motions on a much slower time scale (0.2−0.6 ns). Slower motions of $\tau_e$ on the time scale of 0.4−4 ns have also been reported previously for a number of residues in interleukin-1$\beta$ (Clore et al., 1990) and human type-α transforming growth factor (Li & Montelione, 1995).

*Comparison of the Backbone Dynamics in the Presence and Absence of ssDNA.* The binding of ssDNA to the free protein caused significant perturbations in the order parameters for many residues as shown in Figures 5 and 6. The differences between the order parameters ($S^2$) for the free and complexed protein clearly indicate that *the majority of the residues affected by the binding of ssDNA exhibit reduced order parameters or increased mobility as indicated by the positive values* (Figure 5). These residues were found to be located mainly in the $\alpha_1$-helix and two $\beta$-sheets (colored in pink in Figure 6). These results are also reflected in the reduced average order parameters ($S^2$) for the α-helices (0.83 ± 0.03 vs 0.88 ± 0.03) and $\beta$-sheets (0.80 ± 0.05 vs 0.84 ± 0.04) in the complexed vs free protein. The central helix (α1) is located in the center of the two subdomains and beneath the DNA-binding face. The observed increase in the mobility of this helix upon binding to ssDNA suggests that the two subdomains may have greater interdomain motions upon binding to ssDNA.

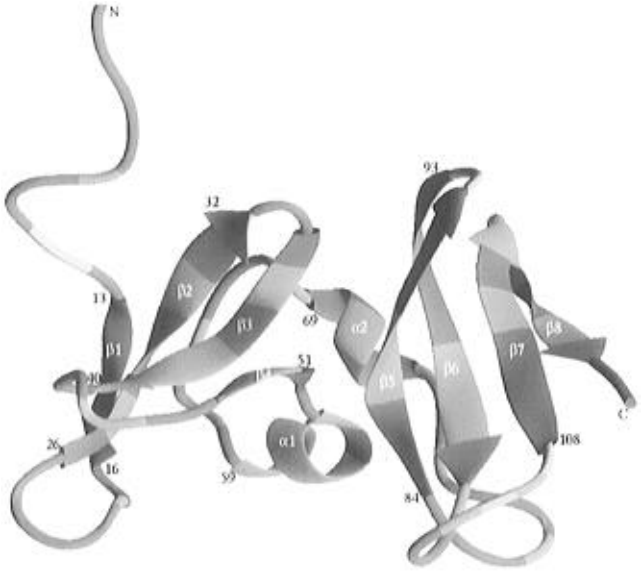


FIGURE 6: Ribbon plot depicting the differential backbone dynamics of the free vs complexed C-terminal domain of *E. coli* topoisomerase I. The ribbon was color-coded as follows: $\Delta S^2 = (S^2_{free} - S^2_{complex})$, for $\Delta S^2 < -0.04$, greenish yellow; for $-0.04 \leq \Delta S^2 \leq 0.04$, cyan; for $\Delta S^2 > 0.04$, pink. For Pro as well as those residues whose relaxation parameters were not determined in either free or complexed protein, the backbone was then color-coded in cyan.

A small number of amides including residues 10, 11, 32, 91−93, 105, 107, and 120 in the complexed protein, however, had increased order parameters or became more restrictive as exhibited by negative values (Figure 5). These residues are located in either a loop or a $\beta$-turn on the DNA-binding face of the molecule (colored in greenish yellow in Figure 6). Furthermore, the exchange broadening factors ($R_{ex}$) were significantly larger in the complexed (2.2 ± 1.7 Hz) vs the free protein (0.5 ± 0.4 Hz) (Figure 3, panels F and C), suggesting that there are significant amounts of slow motions present in the protein/ssDNA complex which result in $^{15}$N line broadening. Such motions could arise from chemical and/or conformational exchange processes.

The increased mobilities upon binding to ssDNA were unexpected on the basis of the results from the previous studies. For staphylococcal nuclease, it was shown that the mean-squared order parameters of the $C^{\gamma}-C^{\delta}$ bond axis increased exclusively in those regions within 10 Å of the inhibitor pdTp and the ligand $Ca^{2+}$ (Nicholson et al., 1992). Similarly, only increased order parameters were observed for the second ion-binding loop in calbindin upon binding of $Cd^{2+}$ (Akke et al., 1993), for the ligand-binding loop (residues 82−87) in the FK506 binding protein upon binding of FK506 (Cheng et al., 1993, 1994), and for the ligand-binding loop in ribonuclease T1 upon binding to its inhibitor 2′GMP (Fushman et al., 1994). On the basis of these previous studies, one would expect to find that the residues involved in interaction with ssDNA in topoisomerase would all exhibit increased order parameters upon binding to ssDNA. However, our results indicate this to be true only for a smaller number of residues, while most residues showed

the opposite trend (Figures 5 and 6). Our observations are more consistent with those from the recent study of the PLC$\gamma$1C SH2 domain (Farrow et al., 1994), where decreased order parameters were observed upon binding to a phosphopeptide.

The changes in order parameters upon ligand binding could be influenced by many factors. In this study, the ligand used (12-mer ssDNA) is much bigger than some of those employed in the previous studies [e.g., small inhibitors and ions (Nicholson et al., 1992; Akke et al., 1993; Fushman et al., 1994) and FK506 (Cheng et al., 1993, 1994)]. Therefore, the binding of the ligand to the protein is expected to affect more residues than the smaller ligands. Furthermore, the 12-mer ssDNA binds with a $K_D$ of $\sim$4 $\mu$M (Yu et al., 1995). This interaction is nonspecific and not dependent on the specific nucleotides. Thus, it is likely that many modes exist for binding which may be accommodated by sliding of the ssDNA along the binding face of the protein. Such a binding process is consistent with the larger exchange broadening factors ($R_{ex}$) observed in the complexed protein. No correlation was observed between the changes of $R_{ex}$ and chemical shifts of the backbone amides upon binding to ssDNA. The complexed and free proteins are in fast exchange on the NMR time scale, which complicates the interpretation of the changes in the dynamic properties of the protein upon binding to ssDNA. However, even for a tighter complex such as PLC$_\gamma$1C SH2/pY1021 peptide (slow exchange on the NMR time scale), a similar decrease in order parameters was observed for most residues of the SH2 domain affected by peptide binding, which was attributed to the possibility that the peptide may exist in multiple conformations when bound (Farrow et al., 1994).

*Conclusions.* We have determined the backbone dynamics of the free and complexed C-terminal domain of *E. coli* topoisomerase I by using the model-free formalism. The N-terminal 11 residues, the C-terminal 2 residues, and the residues located in the $\beta$-turn between strands 2 and 3 are much more mobile than the others in both the free and complexed protein. No obvious motions were observed between the two subdomains in the free protein. However, in the complexed protein, the central $\alpha$1-helix had increased mobility, suggesting that the two domains may experience greater interdomain mobility upon complex formation. By comparison of the mobilities [through the use of order parameters ($S^2$)] of the free vs the complexed protein, protein segments that are sensitive to ligand binding were determined. Our results indicate that the majority of the residues affected by ssDNA binding showed slightly increased mobility and only a small number of loop and turn residues became less flexible upon binding to ssDNA. The nature of the nonspecific interaction between ssDNA and the protein presents many modes for the binding (to ssDNA) which results in a heterogeneous complex which may contribute to the increased flexibility within the complex.

## REFERENCES


Abragam, A. (1961) *Principles of Nuclear Magnetism*, Clarendon Press, Oxford.

Akke, M., Skelton, N. J., Kordel, J., Palmer, A. G., III, & Chazin, W. J. (1993) *Biochemistry 32,* 9832−9844.

Barbato, G., Ikura, M., Kay, L. E., Pastor, R. W., & Bax, A. (1992) *Biochemsitry 31,* 5269−5278.

Beran-Steed, R. K., & Tse-Dinh, Y.-C. (1989) *Proteins: Struct., Funct., Genet. 6,* 249−258.

Cheng, J.-W., Lepre, C. A., Chambers, S. P., Fulghum, J. R., Thomson, J. A., & Moore, J. M. (1993) *Biochemistry 32,* 9000−9010.

Cheng, J.-W., Lepre, C. A., & Moore, J. M. (1994) *Biochemistry 33,* 4093−4100.

Clore, G. M., Driscoll, P. C., Wingfield, P. T., & Gronenborn, A. M. (1990) *Biochemistry 29,* 7387−7401.

Farrow, N. A., Muhandiram, R., Singer, A. U., Pascal, S. M., Kay, C. M., Gish, G., Shoelson, S. E., Pawson, T., Forman-Kay, J. D., & Kay, L. E. (1994) *Biochemistry 33,* 5984−6003.

Fushman, D., Weisemann, R., Thuring, H., & Ruterjans, H. (1994) *J. Biomol. NMR 4,* 61−78.

Kay, L. E., Torchia, D. A., & Bax, A. (1989) *Biochemistry 28,* 8972−8979.

Li, Y.-C., & Montelione, G. T. (1995) *Biochemistry 34,* 2408−2423.

Lipari, G., & Szabo, A. (1982a) *J. Am. Chem. Soc. 104,* 4546−4559.

Lipari, G., & Szabo, A. (1982b) *J. Am. Chem. Soc. 104,* 4559−4570.

Marion, D., Ikura, M., Tcshudin, R., & Bax, A. (1989) *J. Magn. Reson. 85,* 393−399.

Messerle, B. A., Wider, G., Otting, G., Weber, C., & Wüthrich, K. (1989) *J. Magn. Reson. 85,* 608−613.

Nicholson, L. K., Kay, L. E., Baldisseri, D. M., Arango, J., Young, P. E., Bax, A., & Torchia, D. A. (1992) *Biochemistry 31,* 5253−5263.

Palmer, A. G., III, Rance, M., & Wright, P. E. (1991) *J. Am. Chem. Soc. 113,* 4371−4380.

Peng, J. W., & Wagner, G. (1992a) *J. Magn. Reson. 98,* 308−332.

Peng, J. W., & Wagner, G. (1992b) *Biochemistry 31,* 8571−8586.

Powers, R., Clore, G. M., Stahl, S. J., Wingfield, P. T., & Gronenborn, A. (1992) *Biochemistry 31,* 9150−9157.

Shaka, A. J., Keeler, J., Frenkiel, T., & Freeman, R. (1983) *J. Magn. Reson. 52,* 335−338.

Stone, M. J., Fairbrother, W. J., Palmer, A. G., III, Reizer, J., Saier, M. H., Jr., & Wright, P. E. (1992) *Biochemistry 31,* 4394−4406.

Tse-Dinh, Y.-C. (1994) *Adv. Pharmacol. 29A,* 21−37.

Yu, L., Zhu, C.-X., Tse-Dinh, Y.-C., & Fesik, S. W. (1995) *Biochemistry 34,* 7622−7628.

Zhu, C.-X., Samuel, M., Pound, A., Ahumada, A., & Tse-Dinh, Y.-C. (1995) *Biochem. Mol. Biol. Int. 35,* 375−385.

Zink, T., Ross, A., Luers, K., Cieslar, C., Rudolph, R., & Holak, T. A. (1994) *Biochemistry 33,* 8453−8463.


BI960507F